



OPEN ACCESS

EDITED BY
Zhiwei Ji,
Nanjing Agricultural University, China

REVIEWED BY
Lin Yuan,
Qilu University of Technology, China
Kexin Huang,
Xidian University, China

*CORRESPONDENCE
Tushuai Li,
tushuaili@jiangnan.edu.cn

SPECIALTY SECTION
This article was submitted to
Neurogenomics,
a section of the journal
Frontiers in Genetics

RECEIVED 07 May 2022
ACCEPTED 06 July 2022
PUBLISHED 06 September 2022

CITATION
Zhang N, Zhang J, Liu Z and Li T (2022),
Identification of signaling pathways
associated with achaete-scute
homolog 1 in glioblastomas through
ChIP-seq data bioinformatics.
Front. Genet. 13:938712.
doi: 10.3389/fgene.2022.938712

COPYRIGHT
© 2022 Zhang, Zhang, Liu and Li. This is
an open-access article distributed
under the terms of the [Creative
Commons Attribution License \(CC BY\)](#).
The use, distribution or reproduction in
other forums is permitted, provided the
original author(s) and the copyright
owner(s) are credited and that the
original publication in this journal is
cited, in accordance with accepted
academic practice. No use, distribution
or reproduction is permitted which does
not comply with these terms.

Identification of signaling pathways associated with achaete-scute homolog 1 in glioblastomas through ChIP-seq data bioinformatics

Na Zhang¹, Jie Zhang², Zhihong Liu³ and Tushuai Li^{4,5*}

¹School of Food and Bioengineering, Xuzhou University of Technology, Jiangsu, Xuzhou, China, ²School of Biology and Food Engineering, Changshu Institute of Technology, Jiangsu, Suzhou, China, ³The State Key Laboratory of Pharmaceutical Biotechnology, Medical School, School of Life Sciences, Nanjing University, Nanjing, Jiangsu, China, ⁴School of Food Science and Technology, Jiangnan University, Wuxi, Jiangsu, China, ⁵Wuxi School of Medicine, Jiangnan University, Wuxi, Jiangsu, China

Background: Achaete-scute homolog 1 transcription factors were important in the differentiation of neuronal-like glioblastoma (GBM) cancer stem cells (CSCs). To gain a better understanding of the role of ASCL1 in GBM, chromatin immunoprecipitation followed by high-throughput sequencing (ChIP-seq) data can be analyzed to construct their gene transcription regulation network.

Methods: GSE87618 was downloaded from the Gene Expression Omnibus, which is a famous database, in the field of biology. The filtered clean reads were mapped to the human genome utilizing the software of bowtie2. Then, differential peak analysis was performed by diffbind. Finally, the annotated gene functions and signaling pathways were investigated by Gene ontology function and kyoto encyclopedia of genes genomes (KEGG) pathway enrichment analysis. Moreover, the protein-protein interaction network (PPI) analysis of genes obtained from ASCL1 was carried out to explore the hub genes influenced by ASCL1.

Results: A total of 516 differential peaks were selected. GO analysis of functions revealed that promoter, untranslated region (UTR), exon, intron, and intergenic genes were mainly enriched in biological pathways such as keratinization, regulation of cAMP metabolic process, blood coagulation, fibrin clot formation, midgut development, and synapse assembly. Genes were mainly enriched in KEGG pathways including pentose phosphate pathway, glycosphingolipid biosynthesis—globo and isoglobo series, ECM-receptor interaction, and adherens junction. In total, 244 nodes and 475 interaction

Abbreviations: ASCL1, achaete-scute homolog 1; BHLH, basic helix-loop-helix; CTNNB1, catenin beta 1; CCHS, congenital central hypoventilation syndrome; CSCs, cancer stem cells; GBMs, glioblastomas; GO, gene ontology; KEGG, kyoto encyclopedia of genes genomes; PPI, protein-protein interaction network; PN, proneural; GSCs, glioblastoma stem cells; FDR, false-positive rate; PCA, principal component analysis; EGFR, epidermal growth factor receptor; SPTAN1, spectrin alpha, non-erythrocytic 1.

pairs were included in the PPI network with the hub genes including *EGFR*, *CTNNB1*, and *SPTAN1*.

Conclusion: *EGFR*, *SPTAN1*, and *CTNNB1* might be the potential down-stream genes of *ASCL1* in GBM development, and *CTNNB1* might make contributions to GBM progression on regulating the cAMP pathway.

KEYWORDS

achaete-scute homolog 1 gene, glioblastomas, bioinformatics, ChIP-seq, signaling pathways

Introduction

Glioblastoma (GBM), as the most common primary malignant brain tumor in adults, is one of the most aggressive and lethal human tumors characterized by a block in cellular differentiation. The median survival can range from 12 to 15 months among patients undergoing the current standard of care treatment involving surgery, chemotherapy, and radiation therapy (Ji et al., 2015; Shabihkhani et al., 2017; Xu et al., 2017; Mortazavi, 2018; Jin et al., 2019). For GBM patients, the disease is hardly diagnosed in the early stage. Meanwhile, recent therapeutic options are limited and prognosis is poor (Berninger et al., 2007). Due to the extremely high malignant grade of GBM, surgical resection combined with radiotherapy and chemotherapy has not changed its malignant progression trend, which is a serious threat to human health. Thus, novel treatment paradigms are urgently needed to improve outcomes. Currently, many efforts are focused on the target therapies, such as traditional small molecule inhibitors, monoclonal antibodies, and immunotherapeutic approaches (Park et al., 2017). These treatment strategies are actively examined in clinical trials and offer an attractive alternation (Shao et al., 2013; Narayanan et al., 2018; Bao et al., 2020). At present, various bioinformatics methods have sprung up, and a large amount of tumor gene expression profile data have become the research direction of tumor precision therapy. Therefore, the study of the glioma gene expression network also has an important theoretical value and practical significance, and its clinical application prospect should not be rested.

ASCL1 is a gene classifier for the pro-neural (PN) transcriptional subgroup of GBM, which plays as a relevant role in the neuronal-like differentiation of glioblastoma stem cells (GSCs). It has been noted that cell-cycle exit and full neuronal specification and differentiation could be induced by *ASCL1* over-expression in neural precursor cells (Barrett et al., 2013). Park *et al.* demonstrated that the transcription factor *ASCL1* was required for GSCs to undergo neuronal lineage differentiation, and GSCs with high *ASCL1* expression levels were responsive to notch pathway inhibitors and important in driving neuronal fate (Kent et al., 2002; Langmead and Salzberg, 2012; Bolger et al., 2014). Furthermore, Narayanan proposed that *ASCL1* might be served as potential subgroup-specific targetable vulnerability in GBM through targeting *NDRG1* (Zhang et al.,

2008; Stark, 2011; Bao et al., 2018; Ji et al., 2019; Bao et al., 2021). These efforts suggest that *ASCL1* plays important roles in neuronal specification. However, the molecular network associated with the roles of *ASCL1* in GBM has not yet been researched.

In order to clarify the regulatory mechanisms of the *ASCL1* in GBM, the data of ChIP-seq were analyzed by utilizing bioinformatics method. The annotated gene functions and signaling pathways were investigated by Gene ontology (GO) function and kyoto encyclopedia of genes genomes (KEGG) pathway enrichment analysis. Moreover, the protein-protein interaction network (PPI) analysis of genes was constructed to explore the hub genes influenced by *ASCL1*.

Materials and methods

Data sources

GSE87618 was the genome occupancy profiling of differential *ASCL1* binding between control and GSC cultures induced to overexpress *ASCL1* after 18 h of doxycycline treatment, which were downloaded from the database of Gene Expression Omnibus (GEO, <http://www.ncbi.nlm.nih.gov/geo/>) (Robinson and Oshlack, 2010). GSE87618 contained data from eight samples, including three *ASCL1* ChIP-seq negative controls (nc1, nc2, nc3), one *ASCL1* ChIP-seq negative control input (nc_input), three *ASCL1* ChIP-seq doxycycline (dox1, dox2, dox3, 18 h of doxycycline treatment), and one *ASCL1* ChIP-seq doxycycline input (dox_input, 18 h of doxycycline treatment). Sra format profile data of GSE87618 were downloaded, and the microarray data were then converted into fastq utilizing fastq-dump (https://trace.ncbi.nlm.nih.gov/Traces/sra/sra.cgi?view=toolkit_doc&f=fastq-dump).

Quality control of sequencing data

In order to filter out the unreliable bases and reads, quality control was performed for the original offline data. Sequencing tape joints were firstly removed. Reads with consecutive masses below 20 at both ends or reads less than 36 nt in length would be removed. Clean reads were obtained by utilizing the tool of Trimmomatic (v3.6) (Yu et al., 2015; Bao et al., 2020).

Sequence alignment

The filtered clean reads were mapped to the human genome (UCSC, hg19), utilizing the software of bowtie 2 (Shannon et al., 2003; Huang et al., 2009; Yu et al., 2012; Szklarczyk et al., 2015). The non-unique mapped reads and low-quality mappings in the results were removed, utilizing default parameters.

Peak calling

Peak signal detection is a key step in the ChIP-seq analysis. MACS2 was used to find the peaks of the enrichment region of trusted sequence (the ASCL1 binding region) from the short sequence alignment results and predict the length of the predicted frag_sizes (Dablander and Hinne, 2019). The default parameters and p -value $< 1e-3$ were set as the screening threshold.

Differential peak analysis

Based on the obtained alignment result and the peak call result, differential peak analysis was performed, utilizing diffbind software (Wang et al., 2008) to obtain differential peak binding to the chromosome due to the expression level of ASCL1 between the ASCL1 ChIP-seq doxycycline group and negative control group. The downstream analysis was performed on an overlap peak in at least three samples, and the number of reads covered by the peak was calculated to obtain the binding affinity matrix. Then, the differential peaks were calculated by edgeR (Du et al., 2015; Tang et al., 2015). The screening thresholds were designed as false-positive rate (FDR) < 0.05 and $|\text{Fold change}| > 2$.

Peak annotation

The differential peaks obtained in the previous step were annotated, utilizing Chipseeker (Rheinbay et al., 2013). A 3 kb (up: 2500 bp down: 500 bp) sequence near the transcription start site (TSS) was selected as a promoter region.

Gene ontology function and kyoto encyclopedia of genes and genomes pathway enrichment analysis

Enriched GO function and KEGG pathway were analyzed on the annotated genes (Zhang et al., 2008). The genes were divided into five categories based on different positions, including promoter, UTR, exon, intron, and intergenic. KEGG pathways and GO functions were analyzed for genes on different positions, respectively, utilizing the tool of Database for Annotation, Visualization and Integrated Discovery (DAVID) based on

hypergeometric test (Azzarelli et al., 2022). The significant threshold was set as p value < 0.05 .

Protein–protein interaction network

The database of Search Tool for Retrieval of Interacting Genes (STRING) is an online database for predicting PPIs (Wang et al., 2021). Utilizing STRING (version 10.0, <http://www.string-db.org/>) database, the PPIs of genes were analyzed. The protein pairs with PPI score > 0.4 were collected. Then, Cytoscape (version: 3.2.0, <http://www.cytoscape.org/>) was used to visualize the predicted PPI network (Gorla et al., 2009; Bhinge et al., 2017; Vue et al., 2020).

Three methods were used to evaluate the centrality of the complex network, including degree centrality (Ackermann et al., 2019), betweenness centrality (Nager et al., 2018), and closeness centrality (Chen et al., 1998). CytoNCA was a cytoscape plugin for the calculation of three topology properties (parameter setting: network is without weight) (Mahesparan et al., 1997; Woods et al., 2022). In the CytoNCA output, the node score represented the role of the protein in the network.

Results

Sequencing data quality control and sequence data comparison result

Table 1 shows the quality of sequencing data. The percentages of bases in all eight samples with Phred values greater than 30 were all more than 99.8%. The results of sequencing data comparison are shown in Table 2, and the mapped rates in different samples were all more than 95%.

Peak call based on the expression level of ASCL1

In total, 4792 peaks were obtained in sample DOX_1, 4176 peaks in DOX_2, 4231 peaks in DOX_3, 1211 peaks in NC_1, 1193 peaks in NC_2, and 733 peaks in NC_3. The doxycycline treatment resulted in a higher expression of ASCL1, and then more peaks were obtained.

Differential peak analysis

The differential peak analysis was performed, and a total of 516 differential peaks were selected. The results of the principal component analysis (PCA) between multiple samples are shown in Figure 1A, and the samples in control and doxycycline treatment group were clustered separately. Differential

TABLE 1 Quality of sequencing output data.

Sample	raw_reads	base_base	clean_read	clean_base	clean_read_QC30 (%)	Gc% (%)
dox1	30270652	3057335852	27858530	2783226852	99.88	42
dox2	28593135	2887906635	26234044	2621375448	99.88	42
dox3	26781109	2704892009	24625563	2461120368	99.89	42
dox_input	33156476	3348804076	31951206	3201740411	99.92	42
nc1	29060175	2935077675	26104377	2609039566	99.88	42
nc2	27823338	2810157138	25390202	2537614866	99.88	42
nc3	28106737	2838780437	25336418	2533215072	99.90	42
nc_input	32015101	3233525201	30780580	3081984505	99.92	43

TABLE 2 Comparison results of sequencing data.

Sample	clean_read	Mapped	Mapped rate (%)	Unique mapped	Unique mapped rate (%)
dox1	27858530	26736498	95.97	23031768	82.67
dox2	26234044	25089241	95.64	21628215	82.44
dox3	24625563	23615202	95.90	20451291	83.05
dox_input	31951206	30733109	96.19	26421023	82.69
nc1	26104377	24943337	95.55	21355241	81.81
nc2	25390202	24294770	95.69	20820887	82.00
nc3	25336418	24320000	95.99	21004213	82.90
nc_input	30780580	29595109	96.15	25423607	82.60

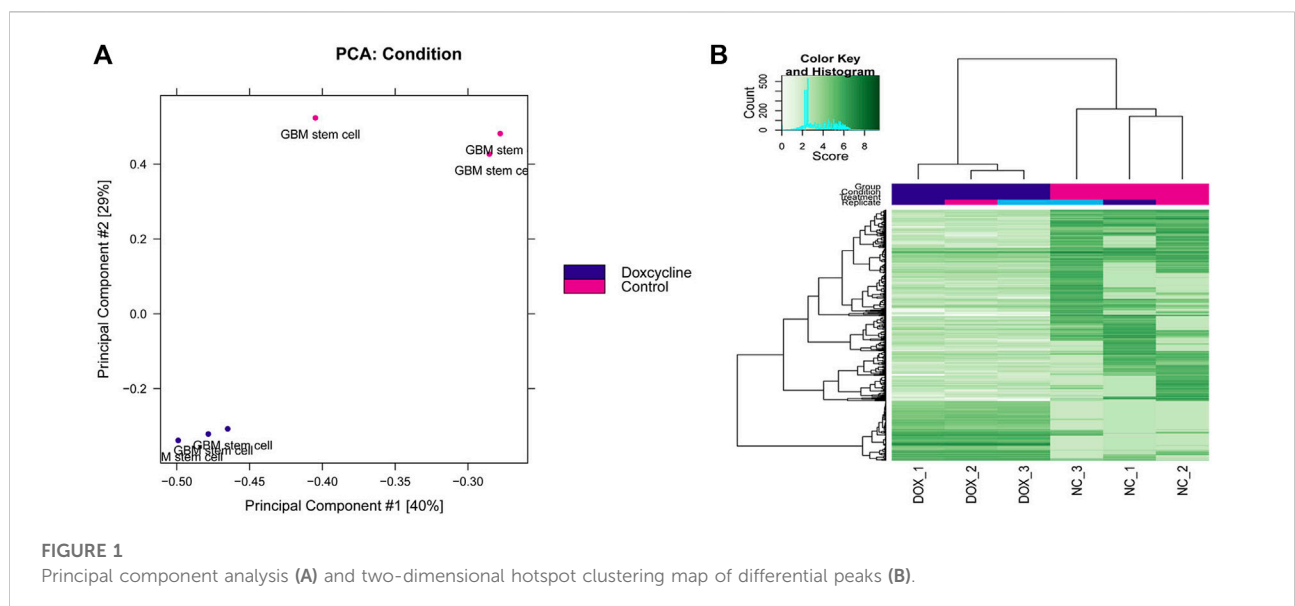
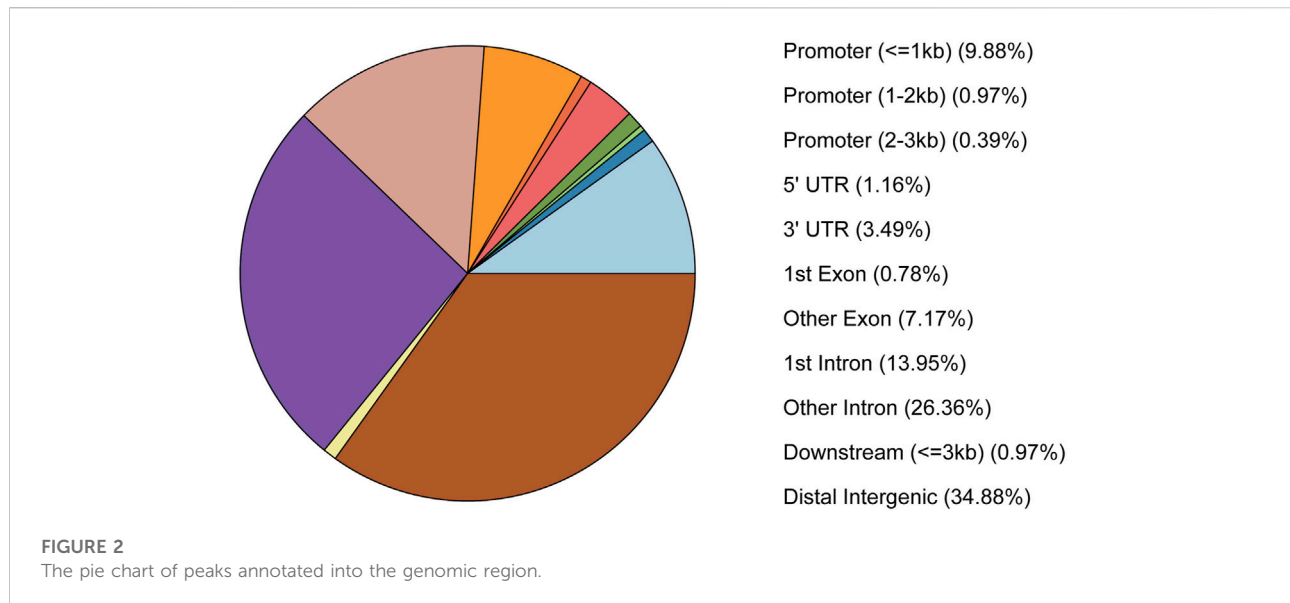


FIGURE 1 Principal component analysis (A) and two-dimensional hotspot clustering map of differential peaks (B).



expression peak hotspot distribution map showed that the profile of differential expression peaks was significantly different in the control and doxycycline treatment group (Figure 1B).

Differential peak annotation

Peaks were annotated by peakseeker, and results showed that 10% peaks were located near the gene promoter, 33% of the peaks were located in the intergenic region, and 40% of the peaks were located in the intron region of the genes (Figure 2).

GO function and KEGG pathway enrichment of genes involved in differential peak annotation

According to the results of the differential peak annotation, the obtained genes were separately subjected to GO functional and KEGG pathway enrichment analysis. As shown in Figure 3A, genes are mainly enriched in biological pathways, such as “odontogenesis of dentin-containing tooth,” “embryonic digit morphogenesis,” and “negative regulation of cell development.” Figure 3B shows that genes are mainly enriched in KEGG pathways, including “starch and sucrose metabolism,” “small cell lung cancer,” and “relaxin signaling pathway.”

Genes were divided into five categories including promoter, UTR, exon, intron, and intergenic. Functional enrichment analysis was further performed, and the results showed that promoter genes were mainly enriched in biological pathways such as keratinization. UTR genes were enriched in the regulation of the cAMP metabolic process. Exon genes were

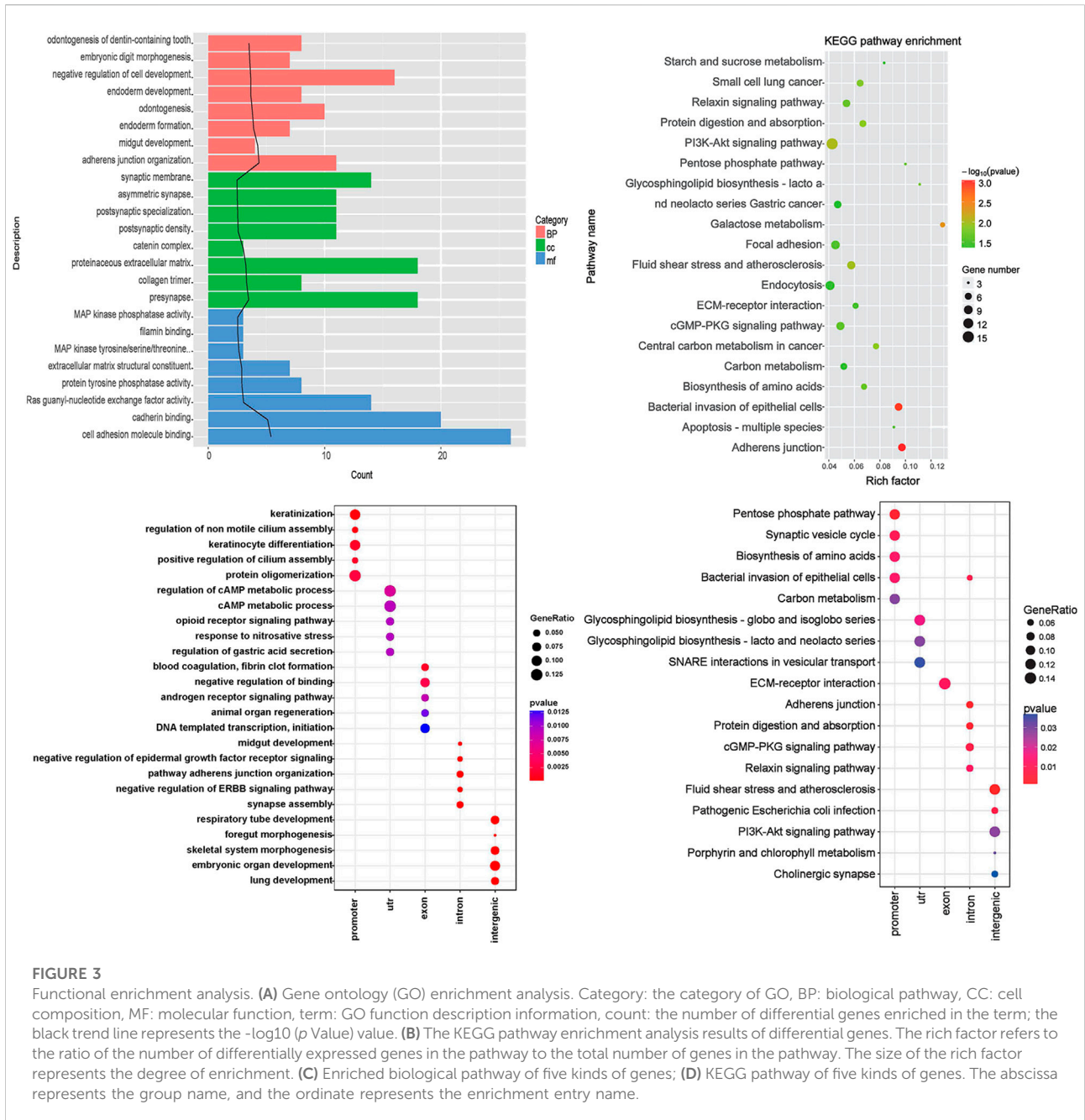
enriched in blood coagulation and fibrin clot formation, intron genes were enriched in midgut development, and intergenic genes were enriched in synapse assembly (Figure 3C). KEGG pathway analysis showed that the significant pathways included pentose phosphate pathway (promoter genes), glycosphingolipid biosynthesis—globo and isoglobo series (UTR genes), ECM–receptor interaction (exon genes), adherens junction (intron genes), and fluid shear stress and atherosclerosis (intergenic genes) (Figure 3D).

PPI network

The PPI network for genes was constructed (Figure 4), and 244 nodes and 475 interaction pairs were included in the network. The top 10 hub nodes based on the degree centrality, betweenness centrality, and closeness centrality are shown in Table 3, such as epidermal growth factor receptor (*EGFR*), catenin Beta 1 (*CTNNB1*), and spectrin alpha, non-erythrocytic 1 (*SPTAN1*).

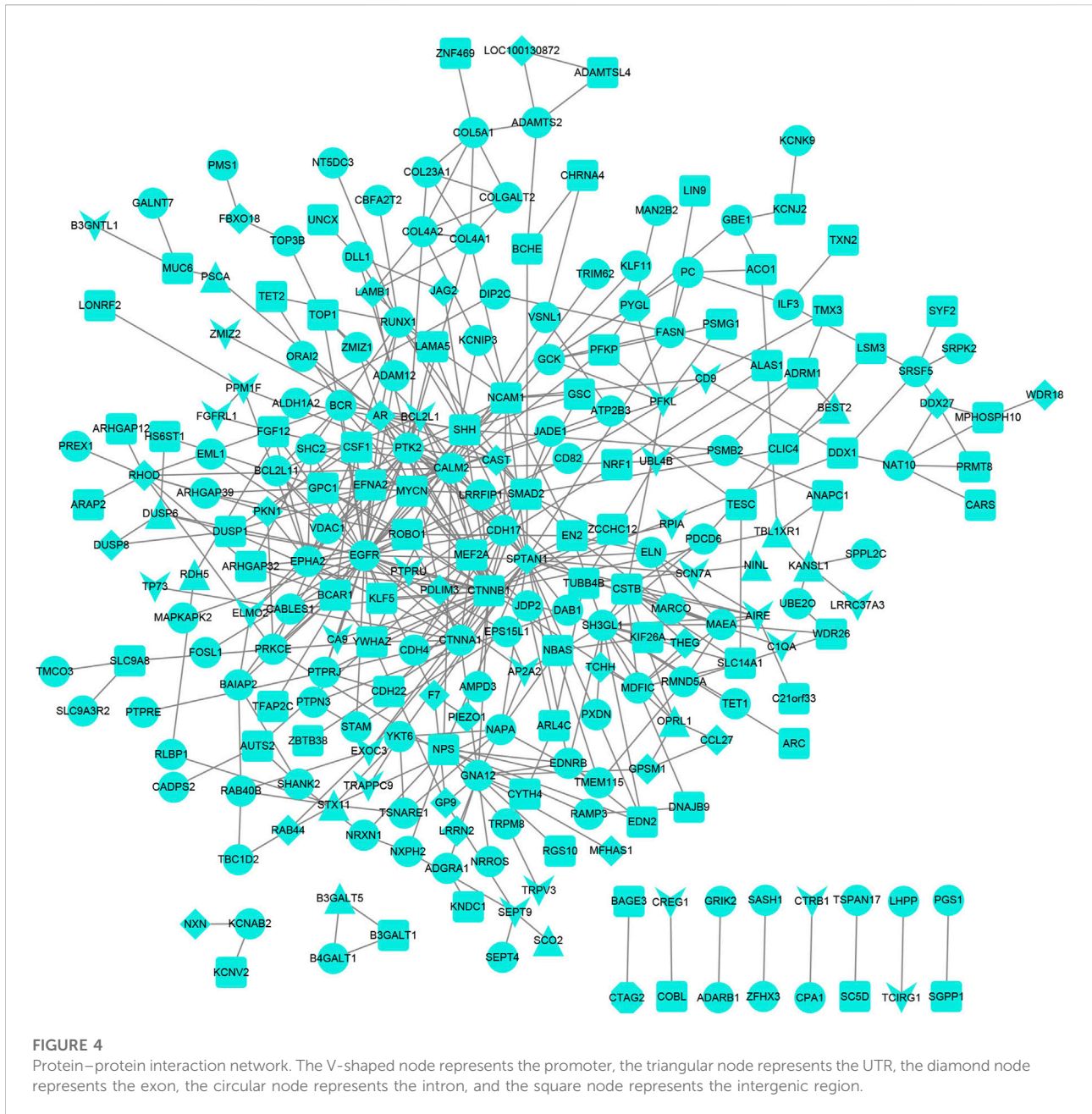
Discussion

GBMs are incurable brain tumors with a high degree of cellular heterogeneity and genetic mutations. For anti-GBM therapies, the loss of proliferation control and unregulated self-renewal would be the most important hard work for clinical treatment. In the context of gliomas, some transcription factors are often expressed and have been shown to function in determining the tumorigenicity and differentiation status of tumor cells. In this study, we focus on ASCL1, a class II basic-helix–loop–helix (bHLH) transcription factor that forms a heterodimer with class I bHLH E-proteins



(such as E47/TCF3) to activate specific target genes. Studies have shown that ASCL1 regulates transcriptional targets that are central to the GBM development. The study of Park *et al.* showed that ASCL1 could control the neuronal fate and suppress tumorigenicity of glioblastoma stem cells by reorganizing chromatin (Park *et al.*, 2017). The study of Rheinbay *et al.* showed that ASCL1 exerts functions in part by repressing an inhibitor of Wnt signaling, DKK1, resulting in increased signaling through this pathway to maintain the tumorigenicity of glioma cells (Shannon *et al.*, 2003). ASCL1 phosphorylation and ID2 upregulation are roadblocks to glioblastoma stem cell

differentiation (Wang *et al.*, 2008; Dablander and Hinne, 2019). The study of Tou *et al.* showed that the loss of ASCL1 significantly reduces the proliferation of GBMs induced in the brain of a genetically relevant glioma mouse model, resulting in extended survival times, illustrating an important role for ASCL1 in controlling the proliferation of GBM (Du *et al.*, 2015). In our study, a total of 516 differential peaks between ASCL1 overexpressed GSC samples and negative controls were screened. GO analysis of functions revealed that the genes annotated on differential peaks were mainly associated with biological pathways such as keratinization, regulation of cAMP



metabolic process, blood coagulation, fibrin clot formation, midgut development, and synapse assembly. Genes were mainly enriched in KEGG pathways including pentose phosphate pathway, glycosphingolipid biosynthesis—globo and isoglobo series, ECM–receptor interaction, adherens junction, and fluid shear stress and atherosclerosis. The PPI network with 244 nodes and 475 interaction pairs was constructed including the hub genes such as *EGFR*, *CTNNA1*, and *SPTAN1*.

The gene expression was mediated by ASCL1 binding to chromatin. In particular, a member of the basic helix–loop–helix (BHLH) family of transcription factors was encoded by ASCL1,

and the protein was important in the neuronal differentiation, olfactory, and autonomic neuron generation. In our study, a regulation network associated with ASCL1 was constructed based on ChIP-seq data. In PPI network, *EGFR*, *CTNNA1*, and *SPTAN1* were hub genes. In lung adenocarcinomas patients, EGFR mediates the activation of RET with neuroendocrine differentiation characterized by ASCL1 expression, implicating that EGFR is a key regulator of RET (Tang et al., 2015). ASCL1 function is an upstream regulator of the Ret Proto-Oncogene, so combined with our findings, we speculate that in GBM, ASCL1 may mediate RET activation

TABLE 3 The top 10 hub nodes in the protein–protein interaction network.

name	Degree	name	Betweenness	name	Colseness
EGFR	41	CTNNB1	13460.64851	CTNNB1	0.041263
CTNNB1	33	CALM2	11008.59049	EGFR	0.041179
SPTAN1	27	SPTAN1	10851.35589	SPTAN1	0.041117
CALM2	27	EGFR	10807.95974	CALM2	0.041117
PTK2	17	GNA12	4305.269611	PTK2	0.040772
SH3GL1	17	DDX1	3878.215375	AR	0.040772
SHH	16	PTK2	3480.394513	SHH	0.040669
CTNNA1	15	AR	3439.149015	BCL2L1	0.040649
AR	14	SHH	3354.04941	MYCN	0.040602
NCAM1	13	SH3GL1	2918.910619	CTNNA1	0.040595
GNA12	13	NPS	2559.36073	CDH17	0.04048
EPHA2	12	NCAM1	2169.773138	YWHAZ	0.040412
BCL2L1	10	TBL1XR1	2112.331093	NCAM1	0.040406
SMAD2	10	NAT10	1869.07619	SMAD2	0.040352
MYCN	10	FASN	1813.87283	MEF2A	0.040319

through EGFR, thereby affecting tumor progression. The protein encoded by *SPTAN1* has been implicated in DNA repair and cell cycle regulation. Meanwhile, this gene was involved with the RET signaling pathway (Rheinbay et al., 2013). Ackermann *et al.* demonstrated a close relationship between low *SPTAN1* expression and tumor progression and metastasis in colorectal cancers (Azzarelli et al., 2022). Although no direct evidence has shown the association between *ASCL1* and the genes such as *EGFR* and *SPTAN1* in GBM, the data revealed its potential value as an important downstream gene of *ASCL1* in GBM.

It has been reported that WNT-CTNN1B signaling plays important roles in promoting cancer cell proliferation and stemness, and Nager *et al.* showed that silencing CTNN1B could decrease cell viability and induce GBM cell apoptosis (Wang et al., 2021). In malignant gliomas, previous evidence showed that protein kinase (PKA) activation was correlated with decreased proliferation, increased differentiation, and apoptosis induction by increasing cAMP levels or directly by cAMP analogues (Vue et al., 2020). Regulation of the cAMP metabolic process was involved in the GO enrichment function in GBM. Together with the data presented herein, there is a growing body of evidence suggesting a role of CTNN1B in GBM progression based on regulating the cAMP pathway. An uncontrolled cell proliferation and infiltrative growth within the brain were the main characteristics in malignant human gliomas. The conjunction with vascular elements has specific interactions between tumor cell surface receptors and specific ECM, which induced an extensive tumor cell movement along blood vessels (Bhinge et al., 2017). Enhancing *ASCL1* activity in a neurogenic environment both increases binding at

endogenous *ASCL1* sites and also results in additional binding to new low affinity sites that favors neuronal differentiation (Gorla et al., 2009). Our data showed that the ECM–receptor interaction and pentose phosphate pathways were dysregulated by *ASCL1* overexpression in GSCs.

Our data provide a genome-wide view of gene regulation by *ASCL1* signaling in GBM, and we showed important roles of hub genes influenced by *ASCL1*. However, there are some limitations that should be noted. The data were all analyzed by the method of bioinformatics, and the potential functional enrichment of genes should be further researched by clinical research. Furthermore, only three *ASCL1* ChIP-seq negative controls and three *ASCL1* ChIP-seq doxycyclines were enrolled in the analysis. It should not be denied that the background of GBM patients varied from each other. Thus, the conclusion should be verified by further systematical analysis.

In summary, we constructed a regulation network for the *ASCL1* role involved in neurogenic gene expression program activation in GBM. Our data revealed that *EGFR* and *SPTAN1* were the potential downstream genes of *ASCL1* in the GBM development, and CTNN1B might take part in GBM progression based on regulating the cAMP pathway. However, the conclusion should be further verified by experimental data.

Data availability statement

The original contributions presented in the study are included in the article/supplementary material; further inquiries can be directed to the corresponding author.

Author contributions

NZ and JZ designed the experiments of this work. ZL collected the data and dealt with the figures and tables in this work. NZ and TL edited the article.

Funding

This work was supported by the Major Basic Research Project of the Natural Science Foundation of the Jiangsu Higher Education Institutions (Nos. 21KJB360022, 20KJB330002), the Xuzhou Key Research and Development Project (No. KC20147), the General Program of China Postdoctoral Science Foundation (2022M711369), and the Suzhou Science and Technology Council (SNG201907).

References

- Ackermann, A., Schrecker, C., Bon, D., Friedrichs, N., Bankov, K., Wild, P., et al. (2019). Downregulation of SPTAN1 is related to MLH1 deficiency and metastasis in colorectal cancer. *PLoS One* 14 (3), e0213411. doi:10.1371/journal.pone.0213411
- Azzarelli, R., McNally, A., Dell'Amico, C., Onorati, M., Simons, B., and Philpott, A. (2022). ASCL1 phosphorylation and ID2 upregulation are roadblocks to glioblastoma stem cell differentiation. *Sci. Rep.* 12, 2341. doi:10.1038/s41598-022-06248-x
- Bao, W., Yang, B., Li, Z., and Zhou, Y. (2018). Laipt: Lysine acetylation site identification with polynomial tree. *Int. J. Mol. Sci.* 201, 113. doi:10.3390/ijms20010113
- Bao, W., Huang, D. S., and Chen, Y. H. (2020). MSIT: malonylation sites identification tree. *Curr. Bioinforma.* 15, 59–67. doi:10.2174/1574893614666190730110747
- Bao, W., Yang, B., and Chen, B. (2021). 2-hydr_ensemble: Lysine 2-hydroxyisobutyrylation identification with ensemble method. *Chemom. Intell. Lab. Syst.* 215, 104351. doi:10.1016/j.chemolab.2021.104351
- Barrett, T., Wilhite, S. E., Ledoux, P., Evangelista, C., Kim, I. F., Tomashevsky, M., et al. (2013). NCBI GEO: archive for functional genomics data sets--update. *Nucleic Acids Res.* 41, D991–D995. doi:10.1093/nar/gks1193
- Berninger, B., Guillemot, F., and Gotz, M. (2007). Directing neurotransmitter identity of neurons derived from expanded adult neural stem cells. *Eur. J. Neurosci.* 25 (9), 2581–2590. doi:10.1111/j.1460-9568.2007.05509.x
- Bhinge, K., Yang, L., Terra, S., Nasir, A., Muppa, P., Aubry, M. C., et al. (2017). EGFR mediates activation of RET in lung adenocarcinoma with neuroendocrine differentiation characterized by ASCL1 expression. *Oncotarget* 8 (16), 27155–27165. doi:10.18632/oncotarget.15676
- Bolger, A. M., Lohse, M., and Usadel, B. (2014). Trimmomatic: a flexible trimmer for illumina sequence data. *Bioinformatics* 30 (15), 2114–2120. doi:10.1093/bioinformatics/btu170
- Chen, T. C., Hinton, D. R., Zidovetzki, R., and Hofman, F. M. (1998). Up-regulation of the cAMP/PKA pathway inhibits proliferation, induces differentiation, and leads to apoptosis in malignant gliomas. *Lab. Invest.* 78 (2), 165–174.
- Dablander, F., and Hinne, M. (2019). Node centrality measures are a poor substitute for causal inference. *Sci. Rep.* 9 (1), 6846. doi:10.1038/s41598-019-43033-9
- Du, Y., Gao, C., Chen, X., Hu, Y., Sadiq, R., Deng, Y., et al. (2015). A new closeness centrality measure via effective distance in complex networks. *Chaos* 25 (3), 033112. doi:10.1063/1.4916215
- Gorla, L., Mondellini, P., Cuccuru, G., Micciche, F., Cassinelli, G., Cremona, M., et al. (2009). Proteomics study of medullary thyroid carcinomas expressing RET germline mutations: Identification of new signaling elements. *Mol. Carcinog.* 48 (3), 220–231. doi:10.1002/mc.20474
- Huang, da W., Sherman, B. T., and Lempicki, R. A. (2009). Systematic and integrative analysis of large gene lists using DAVID bioinformatics resources. *Nat. Protoc.* 4 (1), 44–57. doi:10.1038/nprot.2008.211
- Ji, Z., Wu, D., Zhao, W., Peng, H., Zhao, S., Huang, D., et al. (2015). Systemic modeling myeloma-osteoclast interactions under normoxic/hypoxic condition using a novel computational approach. *Sci. Rep.* 5, 13291. doi:10.1038/srep13291
- Ji, Z., Zhao, W., Lin, H. K., and Zhou, X. (2019). Systematically understanding the immunity leading to CRPC progression. *PLoS Comput. Biol.* 15, e1007344. doi:10.1371/journal.pcbi.1007344
- Jin, M. C., Wu, A., Xiang, M., Azad, T. D., Soltys, S. G., Li, G., et al. (2019). Prognostic factors and treatment patterns in the management of giant cell glioblastoma. *World Neurosurg.* 128, e217–e224. doi:10.1016/j.wneu.2019.04.103
- Kent, W. J., Sugnet, C. W., Furey, T. S., Roskin, K. M., Pringle, T. H., Zahler, A. M., et al. (2002). The human genome browser at UCSC. *Genome Res.* 12 (6), 996–1006. doi:10.1101/gr.229102
- Langmead, B., and Salzberg, S. L. (2012). Fast gapped-read alignment with Bowtie 2. *Nat. Methods* 9 (4), 357–359. doi:10.1038/nmeth.1923
- Mahesparan, R., Tysnes, B. B., Edvardsen, K., Haugeland, H. K., Cabrera, I. G., Lund-Johansen, M., et al. (1997). Role of high molecular weight extracellular matrix proteins in glioma cell migration. *Neuropathol. Appl. Neurobiol.* 23 (2), 102–112. doi:10.1111/j.1365-2990.1997.tb01192.x
- Mortazavi, S. M. J. (2018). Commentary: geographic variations in the incidence of glioblastoma and prognostic factors predictive of overall survival in US adults from 2004–2013. *Front. Aging Neurosci.* 10, 105. doi:10.3389/fnagi.2018.00105
- Nager, M., Sallan, M. C., Visa, A., Pushparaj, C., Santacana, M., Macia, A., et al. (2018). Inhibition of WNT-CTNBB1 signaling upregulates SQSTM1 and sensitizes glioblastoma cells to autophagy blockers. *Autophagy* 14 (4), 619–636. doi:10.1080/1548627.2017.1423439
- Narayanan, A., Gagliardi, F., Gallotti, A. L., Mazzoleni, S., Cominelli, M., Fagnocchi, L., et al. (2018). The proneural gene ASCL1 governs the transcriptional subgroup affiliation in glioblastoma stem cells by directly repressing the mesenchymal gene NDRG1. *Cell Death Differ.* 26, 1813–1831. doi:10.1038/s41418-018-0248-7
- Park, N. I., Guilhamon, P., Desai, K., McAdam, R. F., Langille, E., O'Connor, M., et al. (2017). ASCL1 reorganizes chromatin to direct neuronal fate and suppress tumorigenicity of glioblastoma stem cells. *Cell Stem Cell* 21 (3), 411. doi:10.1016/j.stem.2017.08.008
- Rheinbay, E., Suvà, M. L., Gillespie, S. M., Wakimoto, H., Patel, A. P., Shahid, M., et al. (2013). An aberrant transcription factor network essential for Wnt signaling and stem cell maintenance in glioblastoma. *Cell Rep.* 3 (5), 1567–1579. doi:10.1016/j.celrep.2013.04.021
- Robinson, M. D., and Oshlack, A. (2010). A scaling normalization method for differential expression analysis of RNA-seq data. *Genome Biol.* 11 (3), R25. doi:10.1186/gb-2010-11-3-r25
- Shabihkhani, M., Telesca, D., Movassaghi, M., Naeini, Y. B., Naeini, K. M., Hojat, S. A., et al. (2017). Incidence, survival, pathology, and genetics of adult Latino Americans with glioblastoma. *J. Neurooncol.* 132 (2), 351–358. doi:10.1007/s11060-017-2377-0

Conflict of interest

The authors declare that the research was conducted in the absence of any commercial or financial relationships that could be construed as a potential conflict of interest.

Publisher's note

All claims expressed in this article are solely those of the authors and do not necessarily represent those of their affiliated organizations, or those of the publisher, the editors, and the reviewers. Any product that may be evaluated in this article, or claim that may be made by its manufacturer, is not guaranteed or endorsed by the publisher.

- Shannon, P., Markiel, A., Ozier, O., Baliga, N. S., Wang, J. T., Ramage, D., et al. (2003). Cytoscape: a software environment for integrated models of biomolecular interaction networks. *Genome Res.* 13 (11), 2498–2504. doi:10.1101/gr.1239303
- Shao, H., Peng, T., Ji, Z., Su, J., and Zhou, X. (2013). Systematically studying kinase inhibitor induced signaling network signatures by integrating both therapeutic and side effects. *PLoS One* 8, 12e80832. doi:10.1371/journal.pone.0080832
- Stark, R. B. G. (2011). DiffBind: Differential binding analysis of ChIP-seq peak data. *Bioconductor*. Available at: <http://bioconductor.org/packages/release/bioc/vignettes/DiffBind/inst/doc/DiffBind.pdf>.
- Szklarczyk, D., Franceschini, A., Wyder, S., Forslund, K., Heller, D., Huerta-Cepas, J., et al. (2015). STRING v10: protein-protein interaction networks, integrated over the tree of life. *Nucleic Acids Res.* 43, D447–D452. doi:10.1093/nar/gku1003
- Tang, Y., Li, M., Wang, J., Pan, Y., and Wu, F. X. (2015). CytoNCA: a cytoscape plugin for centrality analysis and evaluation of protein interaction networks. *Biosystems*. 127, 67–72. doi:10.1016/j.biosystems.2014.11.005
- Vue, T. Y., Kollipara, R. K., Borromeo, M. D., Smith, T., Mashimo, T., Burns, D. K., et al. (2020). ASCL1 regulates neurodevelopmental transcription factors and cell cycle genes in brain tumors of glioma mouse models. *Glia* 68 (12), 2613–2630. doi:10.1002/glia.23873
- Wang, H., Hernandez, J. M., and Van Mieghem, P. (2008). Betweenness centrality in a weighted network. *Phys. Rev. E Stat. Nonlin. Soft Matter Phys.* 77, 046105. doi:10.1103/PhysRevE.77.046105
- Wang, X., Pei, Z., Hossain, A., Bai, Y., and Chen, G. (2021). Transcription factor-based gene therapy to treat glioblastoma through direct neuronal conversion. *Cancer Biol. Med.* 18 (3), 860–874. doi:10.20892/j.issn.2095-3941.2020.0499
- Woods, L. M., Ali, F. R., Gomez, R., Chernukhin, I., Marcos, D., Parkinson, L. M., et al. (2022). Elevated ASCL1 activity creates de novo regulatory elements associated with neuronal differentiation. *BMC Genomics* 23 (1), 255. doi:10.1186/s12864-022-08495-8
- Xu, H., Chen, J., and Qin, Z. (2017). Geographic variations in the incidence of glioblastoma and prognostic factors predictive of overall survival in US adults from 2004–2013. *Front. Aging Neurosci.* 9, 352. doi:10.3389/finagi.2017.00352
- Yu, G., Wang, L. G., Han, Y., and He, Q. Y. (2012). clusterProfiler: an R package for comparing biological themes among gene clusters. *OMICS* 16 (5), 284–287. doi:10.1089/omi.2011.0118
- Yu, G., Wang, L. G., and He, Q. Y. (2015). ChIPseeker: an R/bioconductor package for ChIP peak annotation, comparison and visualization. *Bioinformatics* 31 (14), 2382–2383. doi:10.1093/bioinformatics/btv145
- Zhang, Y., Liu, T., Meyer, C. A., Eeckhoute, J., Johnson, D. S., Bernstein, B. E., et al. (2008). Model-based analysis of ChIP-seq (MACS). *Genome Biol.* 9 (9), R137. doi:10.1186/gb-2008-9-9-r137